REPORT

SOLID-STATE PHYSICS

Anomalously low electronic thermal conductivity in metallic vanadium dioxide

Sangwook Lee,[1,2]* Kedar Hippalgaonkar,[3,4]* Fan Yang,[3,5]* Jiawang Hong,[6,7]* Changhyun Ko,[1] Joonki Suh,[1] Kai Liu,[1,8] Kevin Wang,[1] Jeffrey J. Urban,[5] Xiang Zhang,[3,8,9] Chris Dames,[3,8] Sean A. Hartnoll,[10] Olivier Delaire,[7,11]† Junqiao Wu[1,8]†

In electrically conductive solids, the Wiedemann-Franz law requires the electronic contribution to thermal conductivity to be proportional to electrical conductivity. Violations of the Wiedemann-Franz law are typically an indication of unconventional quasiparticle dynamics, such as inelastic scattering, or hydrodynamic collective motion of charge carriers, typically pronounced only at cryogenic temperatures. We report an order-of-magnitude breakdown of the Wiedemann-Franz law at high temperatures ranging from 240 to 340 kelvin in metallic vanadium dioxide in the vicinity of its metal-insulator transition. Different from previously established mechanisms, the unusually low electronic thermal conductivity is a signature of the absence of quasiparticles in a strongly correlated electron fluid where heat and charge diffuse independently.

In a Fermi liquid, the same quasiparticles that transport charge also carry heat. Therefore, in most normal metals the charge and heat conductivities are related via the Wiedemann-Franz (WF) law: The ratio between the electronic thermal conductivity (κ_e) and the product of electrical conductivity (σ) and absolute temperature (T) is a constant called the Lorenz number, $L = \kappa_e/\sigma T$, typically not very different from the Sommerfeld value $L_0 = (\pi^2/3)(k_B/e)^2 = 2.44 \times 10^{-8}$ W ohm K^{-2} (where k_B is the Boltzmann constant and e is the electron charge). Recently, violations of the WF law have been theoretically predicted (*1*–*4*) or experimentally observed (*5*–*13*) in some electronic systems. However, with one exception observed in a one-dimensional conductor at room temperature (*13*), these violations typically occur at cryogenic temperatures and arise from unconventional phases of matter, strong inelastic scattering of quasiparticles, or semimetal physics. Here we report a drastic breakdown of the WF law at high temperatures, with L smaller than L_0 by almost an order of magnitude, in a strongly correlated metal [vanadium dioxide (VO_2)]. The observed anomalously low electronic thermal conductivity is accompanied by an unusually high electronic thermoelectric figure of merit; tungsten (W) doping causes both properties to partially revert to normal values. The violation of the WF law is attributed to the formation of a strongly correlated, incoherent non-Fermi liquid, in which charge and heat are independently transported by distinct diffusive modes at high temperatures rather than carried by long-lived quasiparticles (*14*, *15*).

We observed the effect in the metallic phase of VO_2 in the vicinity of its metal-insulator transition (MIT). VO_2 undergoes the MIT at 340 K, accompanied by a first-order structural phase transition from the monoclinic insulating (I) phase to the tetragonal metallic (M) phase on heating (*16*). In this work, κ_e is determined by subtracting the phonon (lattice) thermal conductivity (κ_{ph}), obtained by combining first-principles calculations with x-ray scattering measurements, from the measured total thermal conductivity (κ_{tot}). Previously, κ_{tot} of VO_2 has been measured in bulk and thin films with conflicting conclusions. In bulk VO_2, for example, it was reported that κ_{tot} stays constant (*17*) or decreases very slightly (*18*) with increasing T across the MIT. Unknown electronic scattering leading to a possible failure of the WF law in VO_2 was alluded to nearly half a century ago (*17*), but this has not been experimentally or analytically investigated. Recently, however, time-domain thermal reflectance measurements on polycrystalline VO_2 films showed an increase in κ_{tot}, with a magnitude seemingly consistent with the WF law (*19*). Unlike in those measurements, we use single-crystal VO_2 nanobeams, where the single crystallinity and freestanding configuration in our measurements eliminate extrinsic domain and strain effects. Moreover, our sample geometry ensures that both heat and charge flow in the same path along the nanobeam length direction. This is a crucial condition that, if not satisfied, could result in an erroneous determination of κ_e and assessment of the WF law, especially for VO_2, which has an anisotropic crystal structure. The single-crystal VO_2 nanobeams were grown by the previously reported vapor-transport method (*20*–*22*) (see materials and methods, along with figs. S1 and S2). Figure 1A shows a nanobeam bonded to two microfabricated, suspended pads for simultaneous measurements of κ_{tot}, σ, and the Seebeck coefficient (*23*, *24*) (details in materials and methods, as well as figs. S3 and S4). The thermal and electrical contact resistances were determined to be negligible (materials and methods; see also figs. S5 and S6).

The measured κ_{tot} of a representative VO_2 nanobeam is shown in Fig. 1B. Consistent with a previous study on bulk VO_2 (*17*), our nanobeams exhibit very little change in κ_{tot} across the MIT: $\Delta\kappa_{tot} \sim 0.2$ W/m·K. More than five VO_2 nanobeams with different sizes were measured, and all show $\Delta\kappa_{tot}$ at this level or lower (materials and methods and fig. S8). From the measured σ of the nanobeam across the MIT, the expected electronic thermal conductivity (κ_e^0) for conventional Fermi liquid transport can be calculated, assuming that both phases obey the WF law ($L = L_0$). With σ rising from 4.6×10^3 S/m (I phase) to 8.0×10^5 S/m (M phase) (where 1 S = 1 A/V), κ_e^0 exhibits an abrupt jump from nearly zero to 6.9 W/m·K (Fig. 1B). The measured $\Delta\kappa_{tot}$ is less than 3% of κ_e^0 in the M phase. Considering that κ_e^0 alone in the M phase is already greater than the measured κ_{tot}, application of the WF law would imply an unphysical, negative κ_{ph} in the M phase.

To better understand this anomaly, we determined κ_{ph} in both I and M phases (κ_{ph}^I and κ_{ph}^M) by combining first-principles calculations with measurements (details in materials and methods and fig. S9). As a first step, the phonon dispersions were calculated using density functional theory (DFT), as shown in Fig. 2A for both I and M phases. From these dispersions, both the phonon group velocity and lattice specific heat were obtained for different phonon modes and wave vectors. Next, on the basis of anharmonic (umklapp) phonon scattering in a pure bulk sample, a full first-principles calculation (*25*) was performed for the phonon relaxation time in the I phase. In this way, a calculated bulk value of $\kappa_{ph}^{I,bulk} = 6.46$ W/m·K was obtained at $T = 340$ K along the rutile-phase c axis (the nanobeam length direction). To evaluate the final nanobeam phonon thermal conductivity (κ_{ph}^I), Matthiessen's rule was then applied to account for

[1]Department of Materials Science and Engineering, University of California, Berkeley, CA 94720, USA. [2]School of Materials Science and Engineering, Kyungpook National University, Daegu 41566, South Korea. [3]Department of Mechanical Engineering, University of California, Berkeley, CA 94720, USA. [4]Institute of Materials Research and Engineering, A*STAR (Agency for Science, Technology and Research), 2 Fusionopolis Way, Innovis, 08-03, 138634 Singapore. [5]The Molecular Foundry, Lawrence Berkeley National Laboratory, Berkeley, CA 94720, USA. [6]School of Aerospace Engineering and Institute of Advanced Structure Technology, Beijing Institute of Technology, Beijing 100081, China. [7]Materials Science and Technology Division, Oak Ridge National Laboratory, Oak Ridge, TN 37831, USA. [8]Materials Sciences Division, LBNL, Berkeley, CA 94720, USA. [9]Department of Physics, King Abdulaziz University, Jeddah 21589, Saudi Arabia. [10]Department of Physics, Stanford University, Stanford, CA 94305, USA. [11]Department of Mechanical Engineering and Materials Science, Duke University, Durham, NC 27708, USA. *These authors contributed equally to this work. †**Corresponding author. Email: wuj@berkeley.edu (J.W.); olivier.delaire@duke.edu (O.D.)**

impurity and diffuse boundary scattering of phonons. Using the known rectangular cross section, this boundary scattering (*26*) reduces κ_{ph}^{I} from 6.46 W/m·K for the bulk to 6.15 W/m·K for the nanobeam, very close to the experimentally measured value of 5.8 W/m·K (Fig. 1B). The remaining small difference is attributed to scattering from impurities, most probably atomic vacancies as native point defects (supplementary materials).

For the M phase, evaluating the thermal conductivity solely using first-principles calculations is challenging because VO_2 is a strongly correlated electron system that could exhibit both strong electron-electron and electron-phonon interactions (*25*). In addition, phonon scattering has not been successfully calculated with current theoretical techniques. However, previous ab initio molecular dynamics simulations within the framework of DFT were successful in predicting anharmonically renormalized phonon dispersions in the M phase, which were in good agreement with energy- and momentum-resolved inelastic x-ray scattering (IXS) experiments previously reported in (*25*). Using these M-phase first-principles phonon dispersions (Fig. 2A) benchmarked against experiments, together with the phonon scattering rates obtained from the IXS measurements (details in materials and methods and fig. S9), we determined $\kappa_{ph}^{M,bulk} = 5.72$ W/m·K (Fig. 2B), a reduction by 13% from $\kappa_{ph}^{I,bulk}$. Note that this value includes umklapp, electron-phonon scattering, and all other possible scattering of phonons in bulk, defect-free VO_2. With this value of $\kappa_{ph}^{M,bulk}$, using the Matthiessen's rule similar to that used in the I phase, the nanobeam κ_{ph}^{M} for the M phase was obtained. With both boundary and impurity scatterings considered, κ_{ph}^{I} and κ_{ph}^{M} for nanobeams become even closer to each other (Fig. 2B). The electronic thermal conductivity in the M phase (κ_e^M) can then be obtained by subtracting the nanobeam value of κ_e^M from the measured κ_{tot}^{M}. In this way, we obtained $\kappa_e^M = 0.72$ W/m·K and, hence, an effective Lorenz number $L_{eff} = (\kappa_e^M/\kappa_e^0)\cdot L_0 = 0.11L_0$, corresponding to a suppression of L by nearly an order of magnitude. Although the uncertainty of κ_e^M is high compared with κ_e^M itself (~80%), L_{eff}/L_0 is still low, with an upper bound of less than 0.2.

We now show that this effect can be tuned in W-doped VO_2 ($W_xV_{1-x}O_2$) nanobeams. Tungsten was chosen as the dopant because it is known to lower the MIT temperature (T_{MIT}) by detwisting the V-V bonds in the monoclinic I phase (*16*). The effects of W doping on thermal and electrical transport over a wide T range are summarized in Fig. 3, A and B. As can be seen from the electrical conductivity curves, T_{MIT} decreases monotonically with the W-doping fraction x at a rate of ~21 K per atomic % (fig. S1), consistent with previous reports (*21*, *27*). The $W_xV_{1-x}O_2$ nanobeams show a clear jump in κ_{tot} across their MIT, accompanying the abrupt jump in σ, in marked contrast to the behavior of undoped VO_2. To determine L_{eff} in the M phase of $W_xV_{1-x}O_2$, we obtained κ_{ph}^{M} in a similar way as for the undoped VO_2 nanobeams by considering both boundary scattering and the (now substantial) impurity scattering in the I and M phases of $W_xV_{1-x}O_2$.

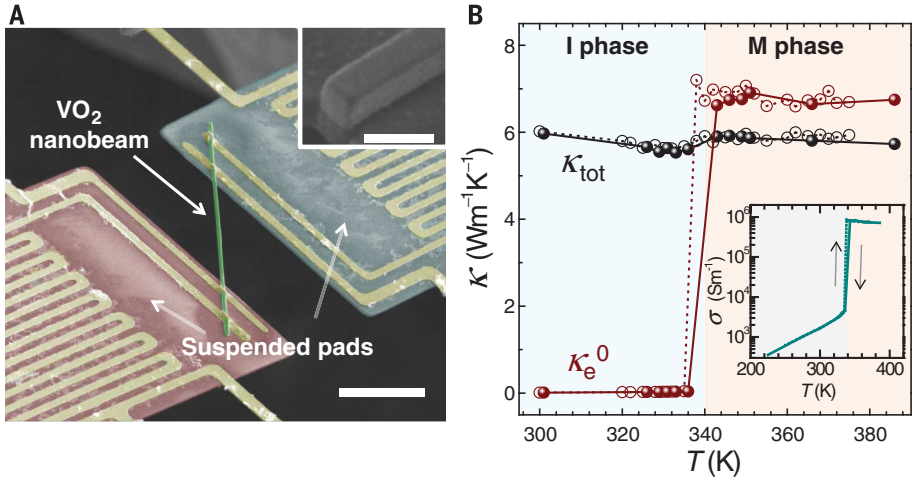

Fig. 1. Thermal conductivity of VO_2 across the metal-insulator transition. (**A**) False-color scanning electron microscopy (SEM) image of a microdevice consisting of two suspended pads bridged by a VO_2 nanobeam. Thermal conductivity is measured by transporting heat from the Joule-heated pad (red) to the sensing pad (blue) through the nanobeam (green). (Inset) SEM image showing the rectangular cross section of a nanobeam. Scale bars: 10 μm (main panel); 500 nm (inset). (**B**) T dependence of measured total thermal conductivity (κ_{tot}) and expected electronic thermal conductivity ($\kappa_e^0 = L_0\sigma T$) of a VO_2 nanobeam. Filled (or open) symbols connected with solid (or dotted) lines are for data collected during heating (or cooling). κ_{tot} has a measurement uncertainty of < 5%, and T has an uncertainty of <0.7%. (Inset) Four-probe electrical conductivity (σ) versus T for the VO_2 nanobeam, used to calculate κ_e^0. Thermal and electrical contact resistances were found to be negligible.

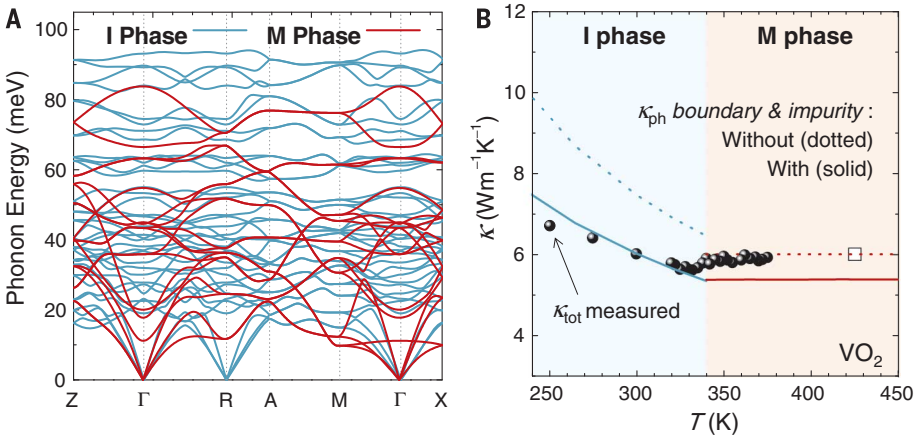

Fig. 2. Separating phonon thermal conductivity from electronic thermal conductivity. (**A**) I- and M-phase phonon dispersions from DFT calculations. To directly compare the phonon energy for the I and M phases, we plotted both dispersions together and used the rutile notation, with the zone boundary R point in the rutile M phase corresponding to the zone center Γ point in the monoclinic I phase. *Z* (0,0,0.5), *R* (0,0.5,0.5), *A* (0.5,0.5,0.5), *M* (0.5,0.5,0), *X* (0.5,0,0). (**B**) Nanobeam κ_{ph} (solid lines) in both I and M phases was calculated by combining κ_{ph}^{bulk} (dotted lines) with boundary and impurity scattering effects. The difference between the measured κ_{tot} and the nanobeam κ_{ph} gives κ_e^M. In the I phase, the DFT framework was used to calculate κ_{ph}^{bulk} according to the DFT-predicted phonon lifetimes; in the M phase, a similar framework was employed to calculate κ_{ph}^{bulk} using the phonon linewidths measured from IXS (*25*) on a bulk sample (open square). In the calculations, the IXS phonon linewidths for the M phase were considered independent of temperature, on the basis of the results reported in (*25*).

It can be seen from Fig. 3C that L_{eff} increases toward L_0 as a function of x (summarized in table S2).

In the $W_xV_{1-x}O_2$ samples, the average W-W distance is estimated to be ~1 nm, larger than our estimated quasiparticle mean free path of electrons in the M phase (~0.5 nm) (materials and methods section S10). With these levels of W doping, the added elastic scattering from the dopants may partially contribute to the rise in L_{eff} for $W_xV_{1-x}O_2$. To elucidate the mechanism behind the vast suppression in L_{eff} and its partial recovery to the normal value with W doping, the Seebeck coefficient (S) of these nanobeams was also measured. The measured S can be used

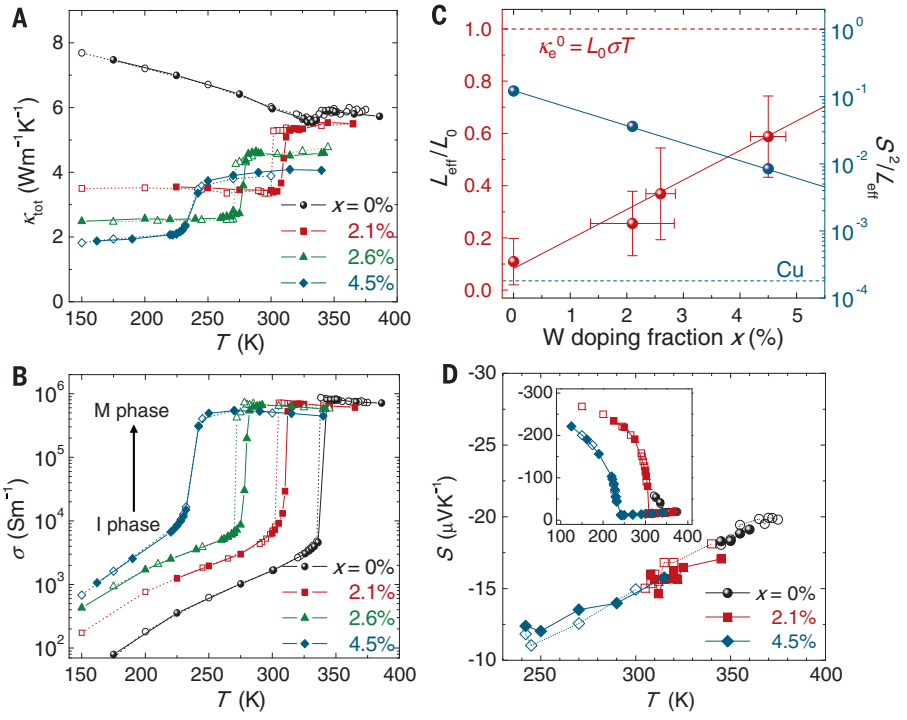

Fig. 3. Breakdown of the WF law from thermal and electrical conductivities of VO_2 and $W_xV_{1-x}O_2$ nanobeams. (**A**) Experimentally measured κ_{tot} of $W_xV_{1-x}O_2$ nanobeams. (**B**) Four-probe electrical conductivity σ versus T for the same set of $W_xV_{1-x}O_2$ nanobeams. T_{MIT} shifts toward lower T with W doping. (**C**) Extracted, normalized Lorenz number as a function of x. L_{eff} is obtained from $(\Delta\kappa_{tot} - \Delta\kappa_{ph})/(\sigma \cdot T)$, and the red solid line is a guide for the eye. Also shown is the M-phase S^2/L_{eff} with x = 0, 2.1, or 4.5% at T_{MIT} of 341, 312, and 240 K, respectively. The blue solid line is a guide for the eye. S^2/L_{eff} for a conventional metallic conductor, copper, is also shown for comparison (blue dashed line). Error bars mostly stem from uncertainties of total thermal conductivities and phonon linewidths. (**D**) Measured Seebeck coefficient S versus T for the M phase of the VO_2 and $W_xV_{1-x}O_2$ nanobeams. (Inset) S over a wider temperature range covering both the I and M phases. In all panels, filled (or open) symbols connected with solid (or dotted) lines represent the data collected during heating (or cooling).

to distinguish different scenarios that all lead to a very small L_{eff}. The dimensionless electronic figure of merit, $S^2/L = S^2\sigma T/\kappa_e$, is ~$10^{-4}$ for a conventional metal such as copper. Our measurements (Fig. 3C) instead show that S^2/L_{eff} = 0.11 for the M phase of VO_2 (summarized in table S2). Such a large value of S^2/L_{eff} for a metal is indicative of nonquasiparticle physics, because the factor k_BT/E_F (where E_F is the Fermi energy) that usually suppresses S is the same factor that suppresses interparticle interactions in a Fermi liquid. This is also supported by consideration of quasiparticle lifetimes (details in the supplementary materials). The quasiparticles, if present, would have a lifetime estimated to be on the order of $\hbar/k_BT$ (where $\hbar$ is Planck's constant h divided by 2π), described as the diffusive "Planckian" limit (*28*), characteristic of strongly interacting metals with T-linear resistivity (*15*). Independently and consistently, the M-phase VO_2 also exhibits a broad Drude peak with a width >~k_BT in the optical conductivity (*29, 30*). Such a short lifetime cannot define meaningfully long-lived quasiparticles (*14*). Another closely related indication of the absence of quasiparticles in VO_2 is that its resistivity is above the Mott-Ioffe-Regel bound; hence, it is a "bad metal" (*31*). A high value of S^2/L_{eff} approaching unity in strongly correlated, nonquasiparticle transport was also revealed in numerical studies using dynamical mean field theory (*32, 33*).

Without long-lived quasiparticles, transport of charge and heat must proceed through collective and independent diffusion (*14*). Hence, the Lorenz ratio of their conductivities has no reason to take the value L_0. Instead, the Lorenz ratio is proportional to the electronic specific heat over charge compressibility. For such systems in the high temperature limit (above the renormalized bandwidth), the temperature dependence of these thermodynamic quantities is relatively insensitive to interactions. Estimates then show that, in general, L_{eff} becomes very small, as the specific heat vanishes more rapidly than the charge compressibility with temperature (*14*) (see supplementary materials). Although L_{eff} numerically recovers toward L_0 with W doping, the linear temperature dependencies of the resistivity (Fig. 3B) and S (Fig. 3D) in the M phase are qualitatively unchanged. The collapse of S with different W doping levels onto the same temperature dependence, as well as the increase of resistivity with doping in the M phase, indicates that the material remains a "bad metal" with W doping, suggesting the continued absence of long-lived quasiparticles. As T_{MIT} is lowered with doping, temperatures close to T_{MIT} (where L_{eff} is measured) are moving away from the asymptotic high-T regime. Therefore, at lower temperatures, although charge and heat diffusions remain independent, one no longer expects $L_{eff} << L_0$; instead, L_{eff} is expected to increase (*14*). A strong electron-phonon interaction may potentially couple κ_{ph} with κ_e, resulting in incomplete separability of κ_{ph} and κ_e in the M phase. However, the electron contribution to the observed κ_{tot} would still remain anomalously low, rendering VO_2 a model system to probe unusual charge behavior in "bad metals." As the decoupled, collective transport of charge and heat occurs universally in incoherent electron fluids, these effects are expected to exist generally in a wide variety of strongly correlated electron materials and can be explored with our experimental methodology. The Lorenz number thus provides a window into the unconventional electronic dynamics of these materials.

REFERENCES AND NOTES

1. C. L. Kane, M. P. A. Fisher, *Phys. Rev. Lett.* **76**, 3192–3195 (1996).
2. K. S. Kim, C. Pépin, *Phys. Rev. Lett.* **102**, 156404 (2009).
3. A. Garg, D. Rasch, E. Shimshoni, A. Rosch, *Phys. Rev. Lett.* **103**, 096402 (2009).
4. R. Mahajan, M. Barkeshli, S. A. Hartnoll, *Phys. Rev. B* **88**, 125107 (2013).
5. Y. Zhang *et al.*, *Phys. Rev. Lett.* **84**, 2219–2222 (2000).
6. N. Doiron-Leyraud *et al.*, *Phys. Rev. Lett.* **97**, 207001 (2006).
7. M. A. Tanatar, J. Paglione, C. Petrovic, L. Taillefer, *Science* **316**, 1320–1322 (2007).
8. H. Pfau *et al.*, *Nature* **484**, 493–497 (2012).
9. Y. Machida *et al.*, *Phys. Rev. Lett.* **110**, 236402 (2013).
10. J. K. Dong, Y. Tokiwa, S. L. Bud'ko, P. C. Canfield, P. Gegenwart, *Phys. Rev. Lett.* **110**, 176402 (2013).
11. R. W. Hill, C. Proust, L. Taillefer, P. Fournier, R. L. Greene, *Nature* **414**, 711–715 (2001).
12. J. Crossno *et al.*, *Science* **351**, 1058–1061 (2016).
13. N. Wakeham *et al.*, *Nat. Commun.* **2**, 396 (2011).
14. S. A. Hartnoll, *Nat. Phys.* **11**, 54–61 (2015).
15. J. A. N. Bruin, H. Sakai, R. S. Perry, A. P. Mackenzie, *Science* **339**, 804–807 (2013).
16. V. Eyert, *Ann. Phys. (Berlin)* **11**, 650–704 (2002).
17. C. N. Berglund, H. J. Guggenheim, *Phys. Rev.* **185**, 1022–1033 (1969).
18. V. N. Andreev, A. V. Chudnovskii, A. V. Petrov, E. I. Terukov, *Phys. Status Solidi, A Appl. Res.* **48**, K153–K156 (1978).
19. D. W. Oh, C. Ko, S. Ramanathan, D. G. Cahill, *Appl. Phys. Lett.* **96**, 151906 (2010).
20. B. S. Guiton, Q. Gu, A. L. Prieto, M. S. Gudiksen, H. Park, *J. Am. Chem. Soc.* **127**, 498–499 (2005).
21. Q. Gu, A. Falk, J. Wu, L. Ouyang, H. Park, *Nano Lett.* **7**, 363–366 (2007).
22. S. Lee *et al.*, *J. Am. Chem. Soc.* **135**, 4850–4855 (2013).
23. P. Kim, L. Shi, A. Majumdar, P. L. McEuen, *Phys. Rev. Lett.* **87**, 215502 (2001).
24. S. Lee *et al.*, *Nat. Commun.* **6**, 8573 (2015).
25. J. D. Budai *et al.*, *Nature* **515**, 535–539 (2014).
26. A. K. McCurdy, H. J. Maris, C. Elbaum, *Phys. Rev. B* **2**, 4077–4083 (1970).
27. X. Tan *et al.*, *Sci. Rep.* **2**, 466 (2012).
28. J. Zaanen, *Nature* **430**, 512–513 (2004).
29. M. M. Qazilbash *et al.*, *Science* **318**, 1750–1753 (2007).
30. M. M. Qazilbash *et al.*, *Phys. Rev. B* **74**, 205118 (2006).
31. V. J. Emery, S. A. Kivelson, *Phys. Rev. Lett.* **74**, 3253–3256 (1995).
32. J. Merino, R. H. McKenzie, *Phys. Rev. B* **61**, 7996–8008 (2000).
33. G. Pálsson, G. Kotliar, *Phys. Rev. Lett.* **80**, 4775–4778 (1998).

ACKNOWLEDGMENTS

This work was supported by the U.S. Department of Energy (DOE) Early Career Award DE-FG02-11ER46796. Parts of this work were performed at the Molecular Foundry, a Lawrence Berkeley National Laboratory user facility supported by the Office of

Science, Basic Energy Sciences, U.S. DOE, under contract DE-AC02-05CH11231, and used facilities of the Electronic Materials Program at LBNL supported by the Office of Science, Basic Energy Sciences, U.S. DOE, under contract DE-AC02-05CH11231. O.D. acknowledges funding from the U.S. DOE, Office of Science, Basic Energy Sciences, Materials Sciences and Engineering Division. C.K. was partially supported by the Tsinghua-Berkeley Shenzhen Institute. K.H. and X.Z. were supported by U.S. DOE, Basic Energy Sciences Energy Frontier Research Center (DoE-LMI-EFRC) under award DOE DE-AC02-05CH11231. K.H. also acknowledges public sector funding from A*STAR of Singapore (M4070232.120) and Pharos Funding from the Science and Engineering Research Council (grant 152 72 00018). J.H. acknowledges support from the National Science Foundation of China (grant 11572040) and the Thousand Young Talents Program of China. Simulation work by J.H. at Oak Ridge National Laboratory was supported by DOE Basic Energy Sciences award DE-SC0016166. Theoretical calculations were performed using resources of the National Supercomputer Center in Guangzhou and the Oak Ridge Leadership Computing Facility. We thank R. Chen, D. F. Ogletree, E. Wong, J. Budai, and A. Said for technical assistance and helpful discussions. J.W. conceived the project; S.L. and J.S. synthesized the materials; S.L., K.H., K.L., and K.W. fabricated the devices; S.L. and K.H. performed the thermal and electrical measurements; C.K. performed Auger electron spectroscopy; F.Y., S.A.H., K.H., C.D., J.J.U., and X.Z. helped with data analysis and theoretical understanding; J.H. and O.D. performed the modeling of thermal conductivity from first-principles phonon dispersions; and all authors contributed to writing the manuscript.

SUPPLEMENTARY MATERIALS

www.sciencemag.org/content/355/6323/371/suppl/DC1
Materials and Methods
Figs. S1 to S11
Tables S1 to S3
References (*34*–*74*)

3 May 2016; accepted 22 December 2016
10.1126/science.aag0410

Anomalously low electronic thermal conductivity in metallic vanadium dioxide

Sangwook Lee, Kedar Hippalgaonkar, Fan Yang, Jiawang Hong, Changhyun Ko, Joonki Suh, Kai Liu, Kevin Wang, Jeffrey J. Urban, Xiang Zhang, Chris Dames, Sean A. Hartnoll, Olivier Delaire and Junqiao Wu (January 26, 2017)

Science **355** (6323), 371-374. [doi: 10.1126/science.aag0410]

Editor's Summary

Decoupling charge and heat transport

In metals, electrons carry both charge and heat. As a consequence, electrical conductivity and the electronic contribution to the thermal conductivity are typically proportional to each other. Lee *et al.* found a large violation of this so-called Wiedemann-Franz law near the insulator-metal transition in VO_2 nanobeams. In the metallic phase, the electronic contribution to thermal conductivity was much smaller than what would be expected from the Wiedemann-Franz law. The results can be explained in terms of independent propagation of charge and heat in a strongly correlated system.

Science, this issue p. 371

Science (print ISSN 0036-8075; online ISSN 1095-9203) is published weekly, except the last week in December, by the American Association for the Advancement of Science, 1200 New York Avenue NW, Washington, DC 20005.